

RADIO OCCULTATION EXPLORATION OF MARS

A. J. KLIORÉ

Jet Propulsion Laboratory, California Institute of Technology, Pasadena, Calif., U.S.A.

Abstract. The radio occultation technique, consisting of the observation of changes in the phase, frequency, and amplitude of a radio signal from a spacecraft as it passes through the atmosphere of a planet before and after occultation, was first applied to measure the atmosphere of Mars with the Mariner IV spacecraft in 1965. The interpretation of these changes in terms of refraction of the radio beam by the neutral atmosphere and ionosphere of the planet provided the first direct and quantitative measurement of its vertical structure and established the surface atmospheric pressure of Mars as lying between 5 and 9 mb. The presence of a daytime ionosphere with a peak electron density of about 10^5 el cm^{-3} was also measured. The Mariner VI and VII spacecraft flew by Mars in 1969 and provided an additional four measurements of the atmosphere and surface radius of the planet. They confirmed the surface pressure values measured by Mariner IV and provided data for a crude estimate of the shape of the planet.

By far the greatest volume of radio occultation information on the atmosphere and surface of Mars was returned by the Mariner IX orbiter which was placed in orbit about Mars in November of 1971. During three occultation episodes in November–December 1971, May–June 1972, and September–October 1972, the Mariner IX mission provided 260 successful radio occultation measurements.

The early measurements, made at the time of the Martian dust storm of 1971, showed greatly reduced temperature gradients in the daytime troposphere, indicating the heating effect of the dust. The temperature gradients that were measured later in the mission, when the atmosphere was apparently free of dust, were still much lower than expected under conditions of radiative-convective balance, indicating that dynamics may play a large part in determining the temperature structure of the Martian troposphere. Temperatures taken at night near the winter poles were consistent with the condensation of carbon dioxide.

The surface atmospheric pressure was observed to vary widely with topography ranging from about 1 mb at the summit of the Middle Spot volcano (Pavonis Mons) to over 10 mb in the North circumpolar region. In the South equatorial region the highest surface pressure of about 9 mb was measured at the bottom of the Hellas basin.

The radius of the planet was measured with accuracies ranging from about 0.25 to about 2.1 km over latitudes ranging from 86° to -80° . These measurements have shown that Mars has pronounced equatorial and north–south asymmetries, which make it difficult to represent its shape by a simple triaxial figure.

The daytime ionosphere measurements indicated that the main ionization peak was similar in behavior to a terrestrial F_1 layer and is probably produced by photoionization of carbon dioxide by solar extreme ultraviolet. Comparison of the heights of the maximum between the early data taken in November–December, 1971, and the Extended Mission of May–June 1972, showed that the lower atmospheric temperatures decreased by about 25%, which is consistent with clearing of the atmosphere.

The experience gained from Mars radio occultation experiments suggests that the quality of data can be significantly improved by such features of the spacecraft radio system as a stable oscillator, dual frequency downlink capability, and a steerable high-gain antenna.

1. Introduction

The technique of spacecraft radio occultation, although less than a decade old, has already produced a large body of results on the atmosphere and topography of Mars. This technique, which is well known and has been described previously, is based on the observation of very small changes in the phase and amplitude of a radio signal from a spacecraft introduced by the effects of refraction by the neutral and electrically charged portions of a planetary atmosphere during the times immediately prior

to and immediately after the occultation of the spacecraft by the planetary body. Such experiments were made possible not only by the advent of interplanetary spacecraft, which brought radio apparatus to the vicinity of planets, but also by the development of very precise spacecraft tracking instrumentation and techniques by the NASA/JPL Deep Space Net. These, in conjunction with advances in celestial mechanics and digital computer technology and techniques, made it possible to unravel the very small effects of refraction in the ionosphere and atmosphere of Mars from the received Doppler frequency data, thus enabling the recovery of the results presented herein.

The refractive effects of an atmosphere upon the propagation of radio waves has been known and understood for some time (Bean and Thayer, 1963). However, the application of this knowledge to spacecraft radio occultation experiments was not proposed until approximately a decade ago (Fjeldbo, 1964; Kliore *et al.*, 1964). The first radio occultation measurement of the atmosphere of Mars was performed with Mariner IV in 1965 (Kliore *et al.*, 1965a). Further measurements were performed with Mariners VI and VII in 1969 (Kliore *et al.*, 1969). These first two opportunities produced six individual measurements. In contrast, the Mariner IX orbiter collected 260 successful individual measurements during 1971 and 1972, which provided the ma-

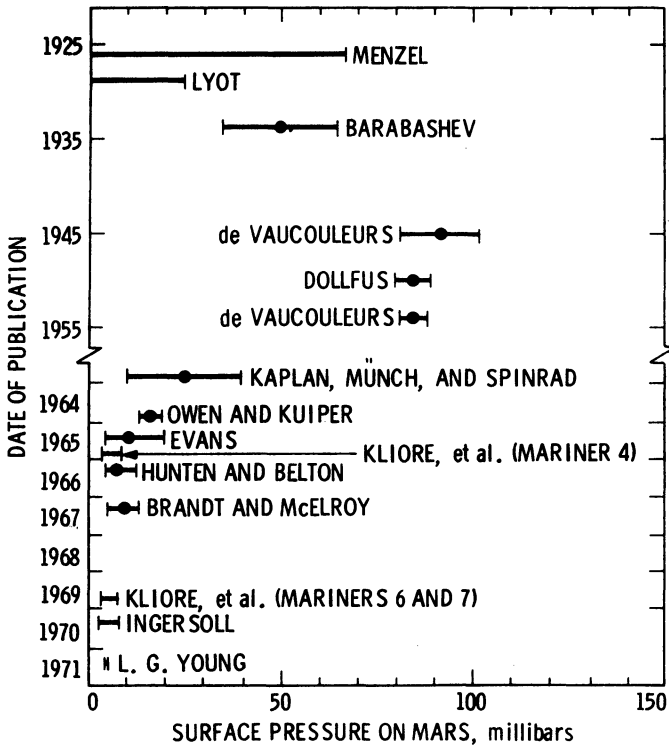


Fig. 1. Historical review of Martian surface pressure estimates.

majority of the important results regarding the atmosphere, ionosphere, and topography of Mars that are discussed in this paper (Kliore *et al.*, 1970a). The Soviet Mars 2 spacecraft was also used to perform a radio occultation experiment (Kolosoov *et al.*, 1972).

The scientific importance of the Mars radio occultation measurements is evident from Figure 1 which displays the range of surface pressure estimates on Mars from a variety of sources. Prior to about 1964, various Earth-based photometric, polarimetric and spectroscopic measurements had indicated a value for the surface pressure of Mars of approximately 85 mb. After 1963, improved spectroscopic techniques were used to drastically reduce the surface pressure estimates, which were confirmed by the results of the Mariner IV Radio Occultation experiment. Since then, a number of re-evaluations of the spectroscopic data as well as radio occultation experiments have indicated a mean surface pressure on Mars of about 5–6 mb, with a wide variation due to topographical height variations of the Martian surface.

2. The Atmosphere

The phase delay data produced by refraction in a planetary atmosphere, together with the precisely known ephemeris of the spacecraft, can be inverted to produce a vertical profile of refractivity as a function of distance from the center of the planet (Fjeldbo and Eshleman, 1968; Kliore, 1972). Such inversion procedures generally assume spherical symmetry in the planetary atmosphere. Using well known relationships from magnetoionic theory, the refractivity in the ionized upper atmosphere can be directly converted to electron density. It should be pointed out that no direct information on the ion species is provided.

In the neutral lower atmosphere a composition must be known or assumed in order to derive other atmospheric parameters from the refractivity. In the case of Mars, this problem is simplified considerably by the fact that no major constituent in addition to carbon dioxide has been discovered by spectroscopic spacecraft observations (Barth *et al.*, 1972). Consequently, all computations of atmospheric parameters are made under the assumption of a carbon dioxide atmosphere. Once the composition has been established, the refractivity can be converted to mass density, and the hydrostatic equation can be integrated vertically to obtain the pressure profile. The temperature profile is then obtained by applying the perfect gas law. It should be noted that an assumption of an upper level initial temperature must be made.

The first two radio occultation measurements of Mars were performed with Mariner IV in July of 1965 (Fjeldbo and Eshleman, 1968; Kliore *et al.*, 1965b, 1968). The entry, or immersion, measurement was made at the latitude of -50.5° in the Electris-Mare Chronium region, and indicated a surface pressure of about 4.5–5.0 mb. It should be pointed out that most of the entry measurements are performed with the spacecraft in the so-called coherent two-way mode, in which the spacecraft transponder coherently transmits back a signal which it receives from the ground station, where the reference frequency is supplied by a very stable frequency standard. Thus

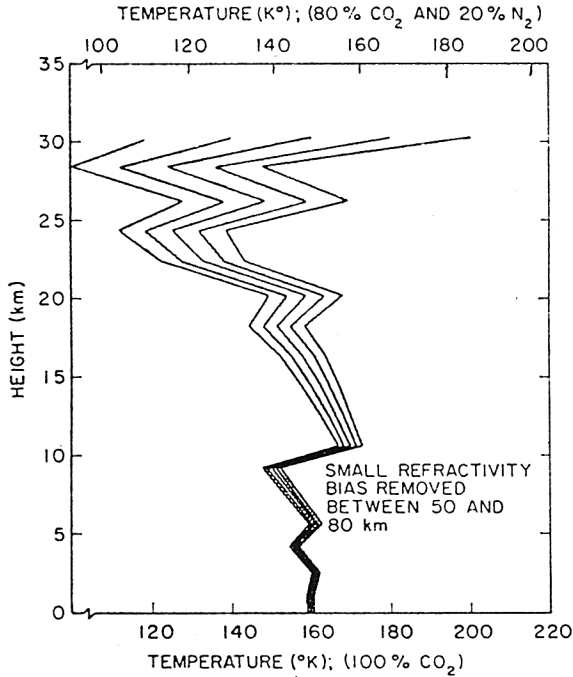


Fig. 2. Mariner IV entry temperature profile for the lower atmosphere measured during Mariner IV entry (from Fjeldbo and Eshleman, 1968).

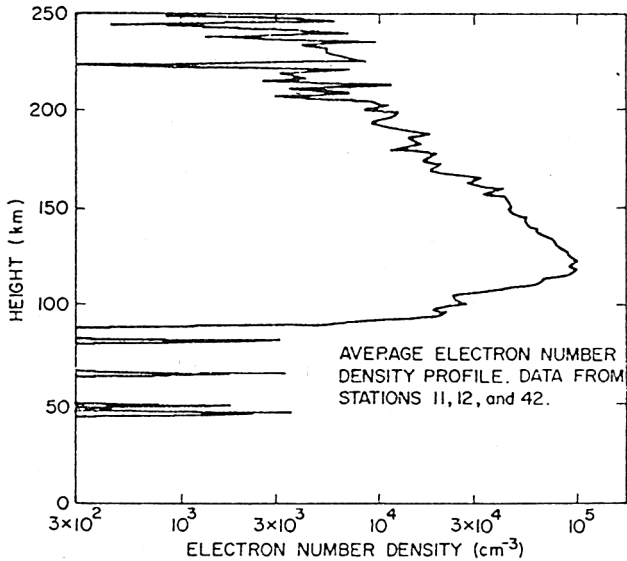


Fig. 3. Ionospheric electron density profile for the Martian upper atmosphere measured during Mariner IV entry (from Fjeldbo and Eshleman, 1968).

the entry data display frequency stability of at least one part in 10^{11} , which is sufficient for the analysis of temperature profiles in the atmosphere. In contrast, during emersion, or the exit phase of occultation, the spacecraft transmitter is referenced to its own crystal oscillator, the short-time stability of which is about an order of magnitude lower, and hence the exit data are not very reliable. In the case of Mariner IV exit, the two-way coherent mode was re-established after the radio beam had traversed about the first 10 km of the atmosphere, and hence two separate kinds of data had to be arbitrarily conjoined during analysis. Nevertheless, it was possible to establish that the surface pressure at the location of the exit measurement at 60° latitude in Mare Acidalium was between 8 and 9 mb. Figure 2 shows a temperature profile derived from the Mariner IV entry data. The five different curves correspond to different choices of the initial temperature and, the temperature profile is remarkably isothermal for the first 30 km. The entry measurement, which was performed approximately at 13:00 h Mars local time in late winter at a solar zenith angle of 67° also produced a profile of the electron density in the ionosphere, which is shown in Figure 3. A main electron peak of about 10^5 el cm^{-3} was observed at an altitude of about 125 km with a subsidiary layer of density 3×10^4 el cm^{-3} at an altitude of about 95 km.

The Mariner IV results established a rather low surface pressure for Mars, which had been predicted from precise Earth-based spectroscopic measurements, and a large disparity between the entrance and exit surface pressures was attributed to local elevation differences. The topside electron scale height of about 22 km was far lower than expected and indicated a plasma temperature of about 280 K if CO_2^+ was the principal ion.

The Mariner VI and VII spacecraft flew by Mars in July and August of 1969 and produced four more occultation measurements (Kliore *et al.*, 1969, 1970b, 1971; Rasool *et al.*, 1970; Fjeldbo *et al.*, 1970). The Mariner VI entry measurement occurred at a latitude of about 4° in the area Meridiani Sinus where a pressure of about 5 mb was measured. The exit occurred at night at about 80° latitude in the area of Boreosyrtis, where the surface pressure was about 6.9 mb. Mariner VII produced a more nearly diametrical occultation, measuring a surface pressure of about 4.2 mb at -68.2° near Hellespontus and about 7.3 mb at 38.1° in the Arcadia-Amazonis area. The temperature profiles derived from the Mariner VI and VII measurements are plotted against pressure in Figure 4. The smooth solid line on the left of the figure is the carbon dioxide saturation curve. The near surface temperature about 250 K indicated at the point of Mariner VI entry was found to be in good agreement with that predicted theoretically on the basis of a surface temperature of about 275 K observed by the infrared radiometer experiment of Mariner VI. In the case of the Mariner VI exit measurement, occurring in the north polar region at night, the CO_2 condensation temperature was reached at an altitude of about 15 km. It was also observed that the average temperature gradients for both of the daytime measurements were of the order of -2.9 to -3.0 K km^{-1} .

Both daytime occultations produced measurements of the structure of the ionized

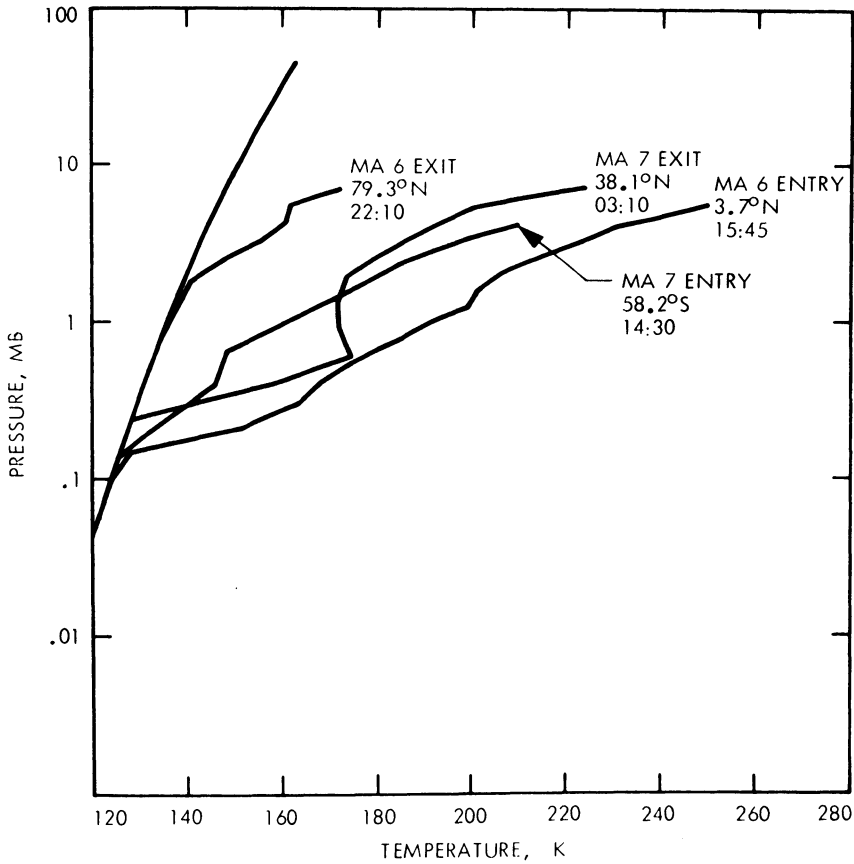


Fig. 4. Mariner VI and VII temperature profiles plotted vs. pressure. The smooth solid line is the carbon saturation curve (from Kliore *et al.*, 1971).

upper atmosphere. The main ionization layer was observed at 135 km altitude with a peak density of approximately $1.7 \times 10^5 \text{ el cm}^{-3}$. A minor layer was observed about 25 km below the main peak. The main ionization peak was interpreted as a F_1 layer consisting primarily of CO_2^+ ions, and the topside plasma temperature was deduced to be 400–500 K, with a neutral density of approximately $10^{10} \text{ m cm}^{-3}$ at an altitude of about 135 km.

By far the largest and most important body of radio occultation data on Mars has been provided by the Mariner IX mission in 1971 and 1972 (Kliore *et al.*, 1972a, b, 1973; Cain *et al.*, 1972, 1973). There were three separate episodes of Mariner IX radio occultations during which data were taken. The first, referred to as the Standard Mission, began with the arrival of Mariner IX at Mars and its injection into orbit on November 14, 1971 and ended on December 23, 1971. The second, called Extended Mission I, began on May 7, 1972 and continued until June 25, 1972. The third, called Extended Mission II, began on September 27, 1972 and continued until October 26,

RADIO OCCULTATION EXPLORATION OF MARS

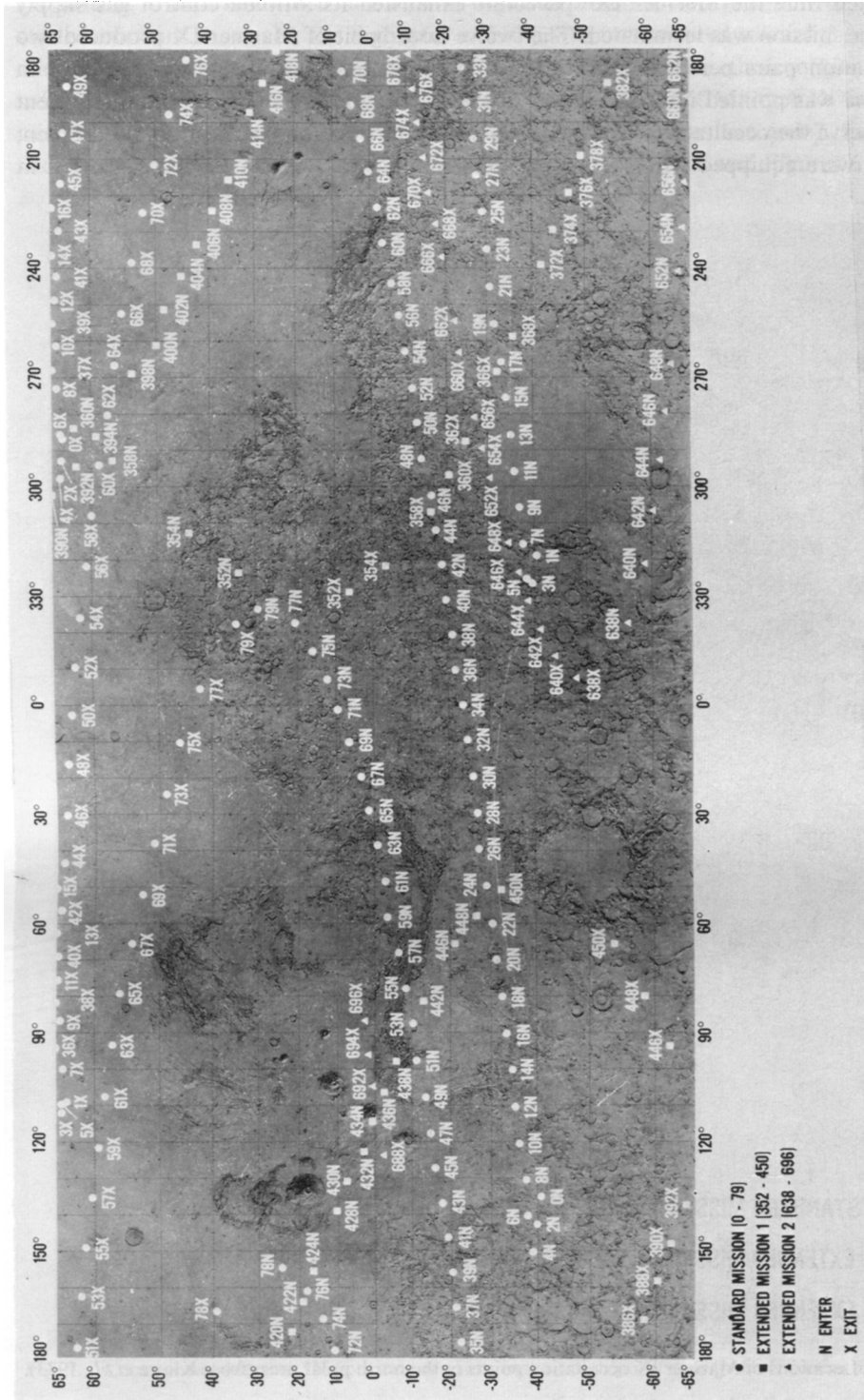


Fig. 5. Locations of all Mariner IX occultation points between the latitudes of ± 65 degrees. The latitudes were computed under the assumption of a spherical planet of radius 3387 km (from Kliore *et al.*, 1973).

at which time the Mariner IX spacecraft exhausted its attitude control gas supply and the mission was terminated. The twelve hour orbit of Mariner IX produced two occultation pairs per day. During the Standard Mission, the spacecraft high gain antenna was pointed in the direction of the Earth, and the signal level was sufficient to observe the occultation from the Deep Space Net stations in Australia and Spain, which were equipped with 26-m diameter antennas, as well as the DSN station at

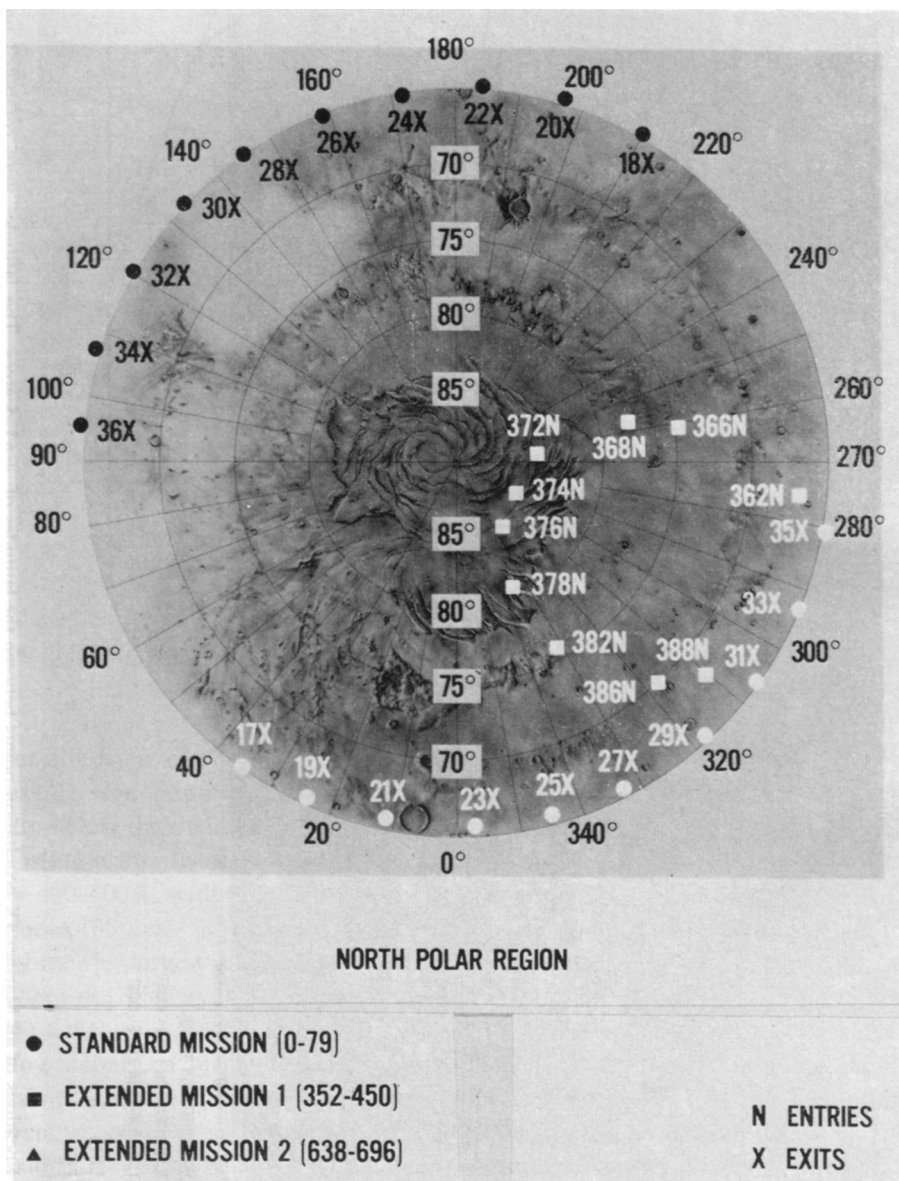


Fig. 6. Locations of Mariner IX occultation points in the north polar area (from Kliore *et al.*, 1973).

describe the locations of occultation points in the north and south polar areas. The locations are labeled with the appropriate orbital revolution numbers, and are identified as being entry or exit measurements with an *N* or an *X*, respectively. The circular marks refer to the Standard Mission (Rev 0–79). The square marks identify measurement points during the Extended Mission I (Rev 352–450) and the triangular marks show the locations of Extended Mission II measurements (Rev 639–696). The relief maps which form the backgrounds of Figures 5, 6 and 7 have been produced by the U.S. Geological Survey from Mariner IX television photographs. During the Standard Mission the geometry was such that the entry measurements were performed mostly in the south equatorial region, at latitudes ranging from about -40° to 20° , and the exit measurements occurred mostly in a band about 65° . The surface atmospheric pressures in the near equatorial region ranged from a high of about 8.9 mb in the depression of Hellas to a low of about 2.8 mb in the Claritas and Tharsis areas, with a mean pressure of about 4.95 mb. The pressures derived from the exit measurements at 65° latitude were much higher, ranging from 7.2 to 10.3 mb, with a mean of 8.9 mb.

All Standard Mission measurements were taken when Mars was covered by a severely obscuring global dust storm. The effect of dust in the atmosphere was apparent in the temperature profiles obtained during the Standard Mission. Figure 8 shows daytime temperature profiles for Revs 0–9. The first three profiles are essentially isothermal, suggesting that large amounts of dust entrained in the atmosphere

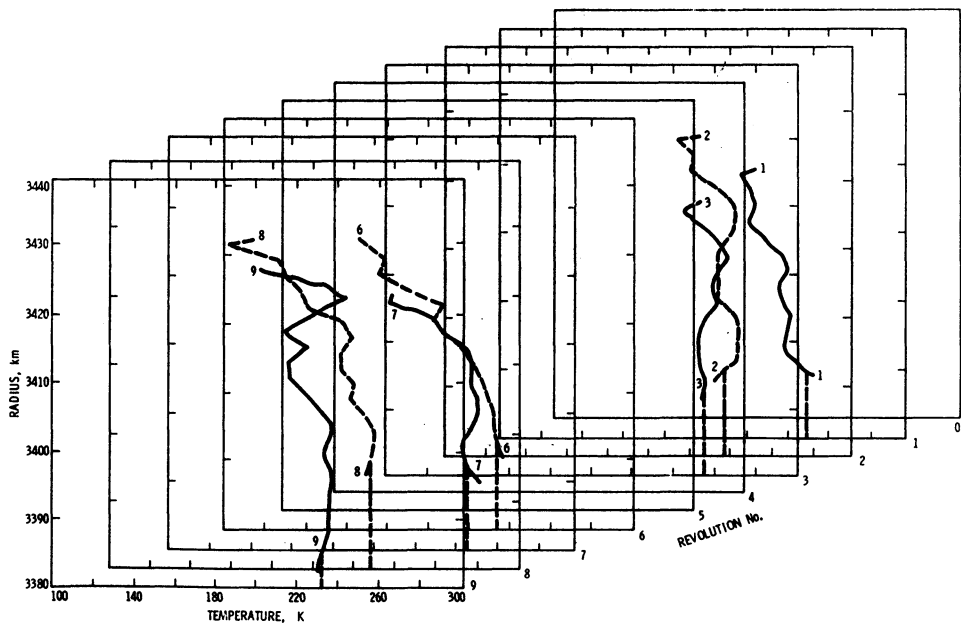


Fig. 8. Temperature profiles derived from Mariner IX entry data for revolutions 0–9 (from Kliore *et al.*, 1972b).

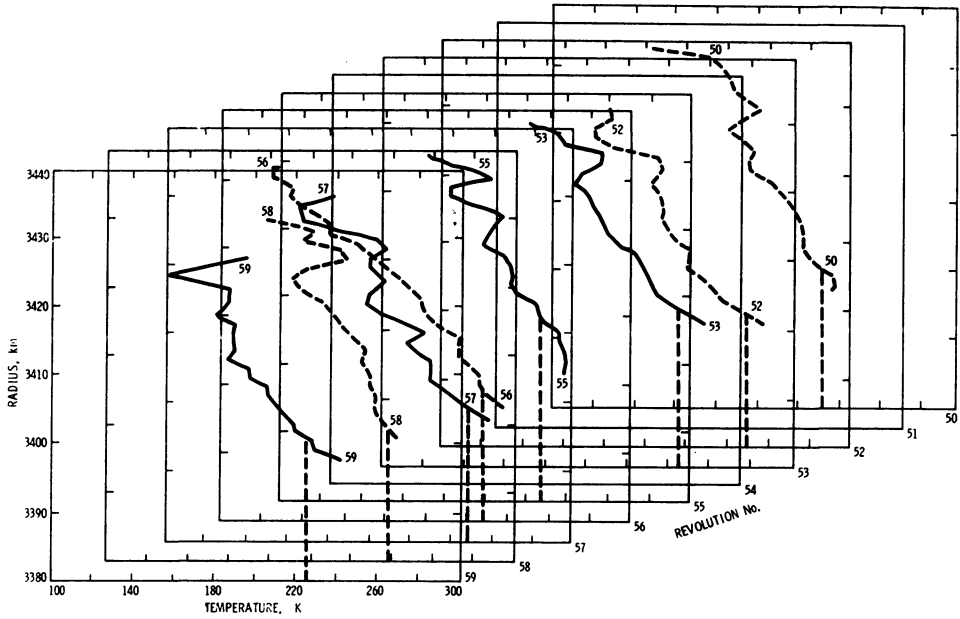


Fig. 9. Temperature profiles from Mariner IX entry occultation data for revolutions 50-59 (from Kliore *et al.*, 1972b).

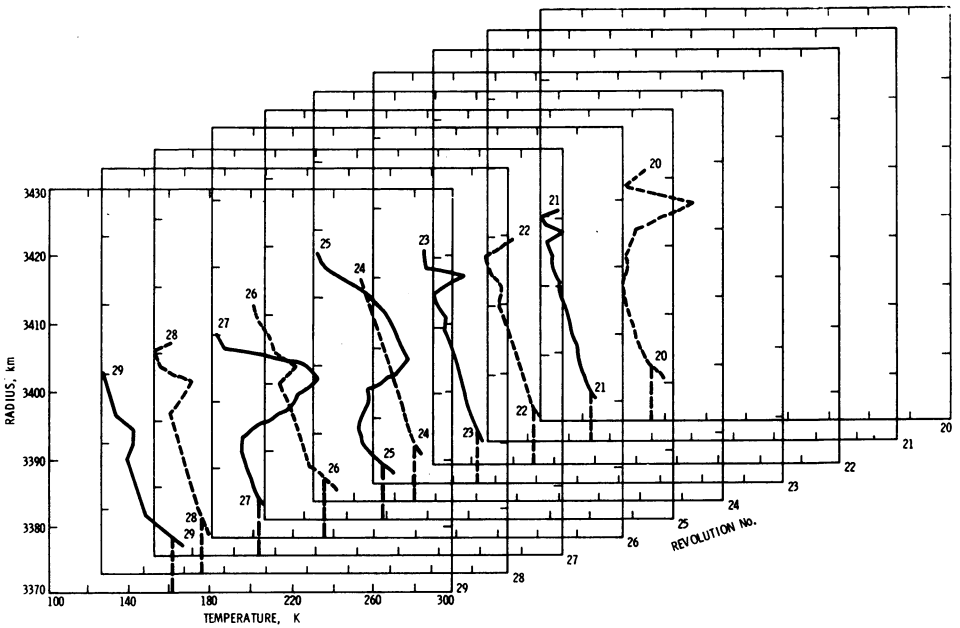


Fig. 10. Temperature profiles derived from exit occultation measurements of Mariner IX for revolutions 20-29 (from Kliore *et al.*, 1972b).

to levels o at least 30 km are absorbing solar radiation, thus heating the upper portions of the troposphere and reducing the temperature of the lower layers. Figure 9 portrays temperature profiles measured in daytime during revolutions 50–59, twenty-five days later. Although Mars was still visually obscured at this time, as evident from television photographs, the atmosphere nevertheless had undergone some degree of clearing and was no longer isothermal in character. The average temperature gradient, however, was still only about -2.5K km^{-1} , which at that time was attributed to the presence of residual dust in the atmosphere.

Standard Mission exit measurements were obtained at around 65° latitude during northern hemisphere mid-winter on Mars, and the temperature profiles derived from these measurements show very low temperatures. Surface temperatures of 150–160 K are indicated, with temperatures reaching the carbon dioxide saturation temperature at altitudes below 10 km. Temperature profiles for exit measurements taken during revolutions 20–29 are shown in Figure 10. The erratic nature of the temperature profiles for revolutions 25 and 27 are most likely caused by instability of the spacecraft oscillator. Measurements of the electron density structure in the daytime ionosphere were obtained for all entry measurements which were taken over a range of

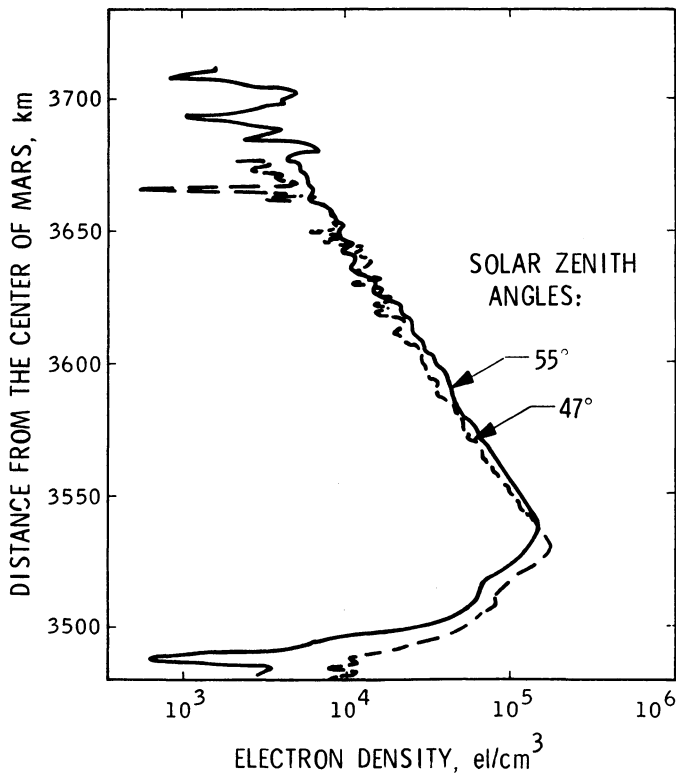


Fig. 11. A comparison of electron density profiles measured by Mariner IX at solar zenith angles of 55 and 47 deg (from Kliore *et al.*, 1973).

a solar zenith angles of 56 to 47 deg. Figure 11 shows two typical electron density profiles, one obtained during revolution 12 at a solar zenith angle of approximately 55°, and the other during revolution 67 at a solar zenith angle of about 47°. As the solar zenith angle gradually decreased in the course of the Standard Mission, the density of ionization increased and the altitude of the maximum became lower.

The second episode of Earth occultations, called Extended Mission I, took place in May and June of 1972 (Kliore *et al.*, 1973; Cain *et al.*, 1973). In contrast to the measurements made during the Standard Mission, these Extended Mission I measurements were remarkable because the latitude coverage ranged from about +86 to -80°, thus providing the first occultation measurements of the north and south polar regions of Mars.

The nine entry measurements obtained at latitudes above 65° indicate surface atmospheric pressures ranging from 4.4 to 7.4 mb, with the average lying about 5.7 mb. The temperature profiles obtained in this region, all taken at low solar elevation angles, did not show appreciable differences in temperature gradients, which were about -2 to -2.5 K km⁻¹. The near surface temperatures, measured directly over the north polar cap, showed temperatures ranging from about 178 K to about 191 K, all substantially above the freezing point of carbon dioxide. Since the surface temperature there was at this time measured to be about 150 K (Kieffer, 1972) by the Infrared Radiometer instrument on Mariner IX, it is strongly suggested that a sharp temperature discontinuity existed in the lower 1 km or so of the atmosphere, which could not be resolved by the radio beam. Some representative temperature profiles from the mid-latitude entry measurements during Extended Mission I are shown in the Figure 12. It is seen that the temperature gradients are quite similar and have an average value of about -2.3 K km⁻¹. The mean temperature gradients

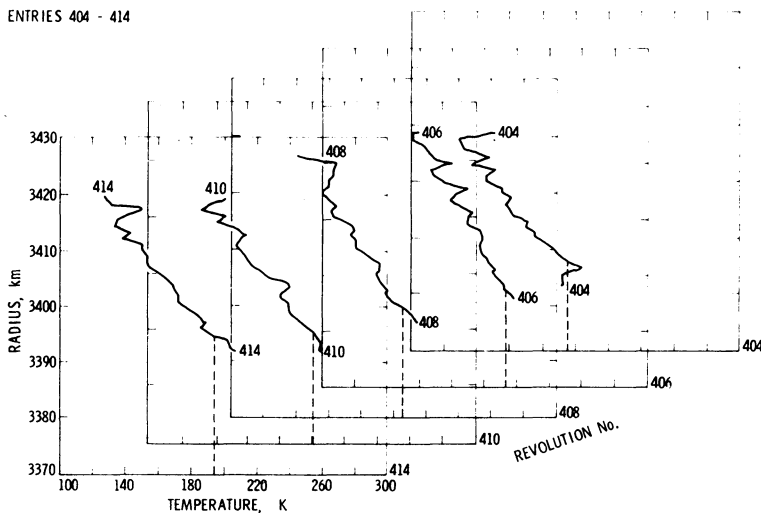


Fig. 12. Temperature profiles from Mariner IX occultation entry measurements during revolutions 404-414 (from Kliore *et al.*, 1973).

in the troposphere for all entry measurements during Extended Mission I range from about 0 to -3.8 K km^{-1} , with no apparent correlation with latitude, Mars local time, or solar elevation angle. These gradients are only slightly steeper than the ones observed during the Standard Mission, when the atmosphere still held a considerable amount of dust, and are far below the theoretical adiabatic gradient of about -5 K km^{-1} (Gierasch and Goody, 1968). Thus it is evident that of all the temperature profiles measured in the Martian atmosphere with Mariners IV, VI, VII and IX, there is not a single case of temperature profile with an adiabatic lapse rate. In fact, they are significantly sub-adiabatic, and the average gradient of about -2.3 K km^{-1} is in very good agreement with gradients deduced for a radiative-dynamical model of the lower atmosphere of Mars described by Stone (1972).

The data taken in the southern polar area consist of one-way exit data, the quality of which was adversely affected by the instabilities of the spacecraft auxiliary oscillator. Most of the deduced surface pressures clustered around 4–5 mb, with temperatures consistent with expectation for nighttime in the winter season at the South Pole.

In the upper atmosphere, data on the structure of the ionosphere was obtained for solar zenith angles greater than 72° during Extended Mission I, in contrast to the $47\text{--}57^\circ$ range covered during the Standard Mission. The observed changes in the

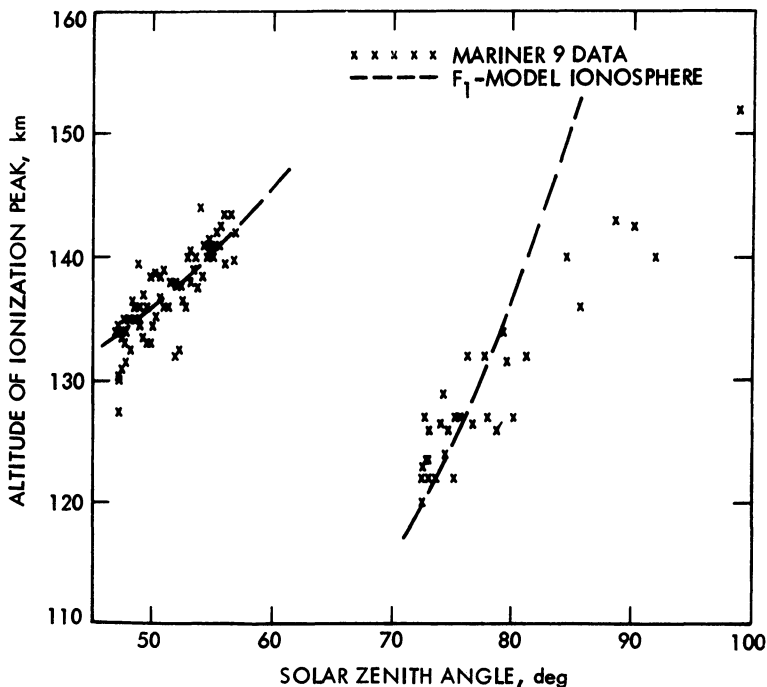


Fig. 13. Variation in the height of the ionosphere peak between the Standard Mission and the Extended Mission I (from Kliore *et al.*, 1973).

altitude of the ionization peak as a function of the solar zenith angle are shown in Figure 13. The discontinuity in the altitude between 57° and 72° is most likely caused by a cooling of the atmosphere between the two sets of measurements. A reduction of the order of 25–30% in the average atmospheric temperature below the ionization peak would be required to explain the entire altitude change, which would be consistent with a clearing of the atmosphere. The model calculation for a F_1 type layer, shown by dashed curve in Figure 13, assumes atmospheric cooling to be the cause of the discontinuity.

The last Mariner IX occultation episode, Extended Mission II, took place in September and October of 1972. In complete contrast to the Standard Mission, the Extended Mission II entry measurements were in a band about -65° latitude, with the exit measurements falling into the mid-latitude regions. Unfortunately, the stability of the spacecraft oscillator had further deteriorated since Extended Mission I, and most of the exit measurements provided unreliable temperature profiles. Some parameters describing the Extended Mission II entry measurements are given in Figure 14. The latitudes are seen to range from about -56 to -67° while the solar elevation angle changes from about $+2$ to -2° and Mars local time ranges from about 09:30 for the early measurements to about 13:00 at the end. Some temperature profiles derived from Extended Mission II entry measurements are shown in Figure 15. The temperatures are all seen to be quite low, with near-surface temperatures ranging from about 140 to 150K, consistent with frozen carbon dioxide on the south polar cap at a time closely approaching southern winter solstice. The data for revolution 648 was taken in the one-way mode and displays the effects of oscillator instability.

The surface pressure readings for Extended Mission II entry measurements are

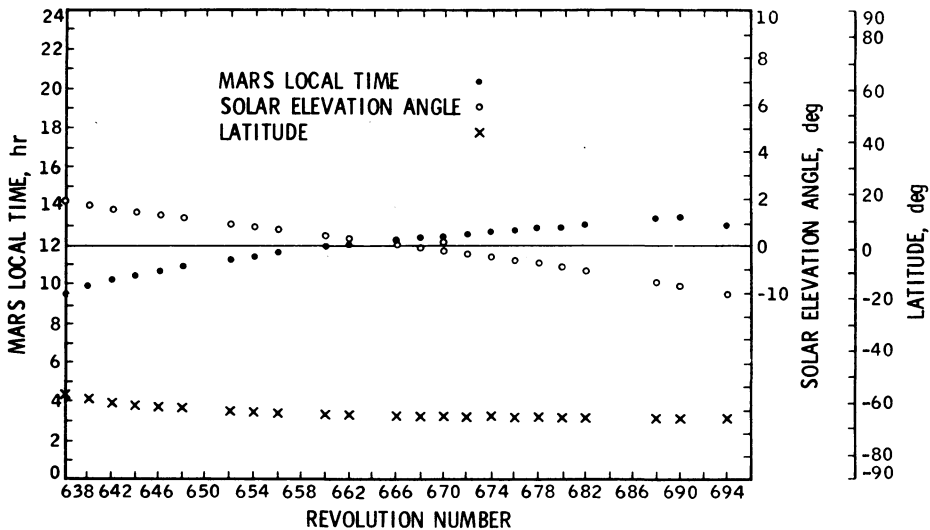


Fig. 14. Latitudes, Mars Local Time, and Solar Illumination angles for entry measurements during Extended Mission II.

shown in Figure 16. The pressures all seem to lie mostly between 4 and 5 mb, in very good agreement with the Extended Mission I exit measurements.

Radio occultation experiments were also performed by the Soviet Mars 2 and Mars 3 spacecraft in 1971 and 1972 (Kolosov *et al.*, 1972). Several measurements of the atmospheric pressure and electron density profiles have been described, generally in agreement with the Mariner IX results.

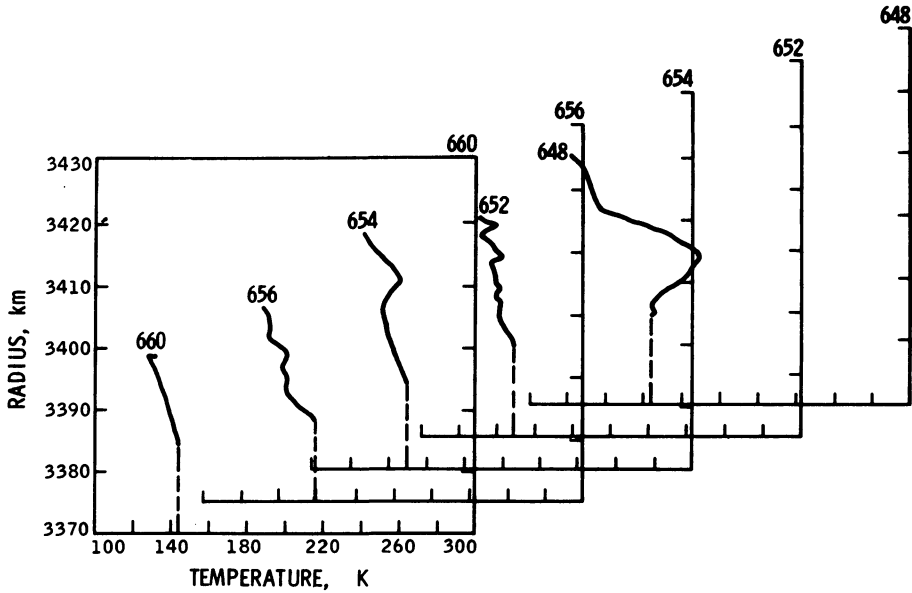


Fig. 15. Temperature profiles from entry occultation measurements during revolutions 648-660.

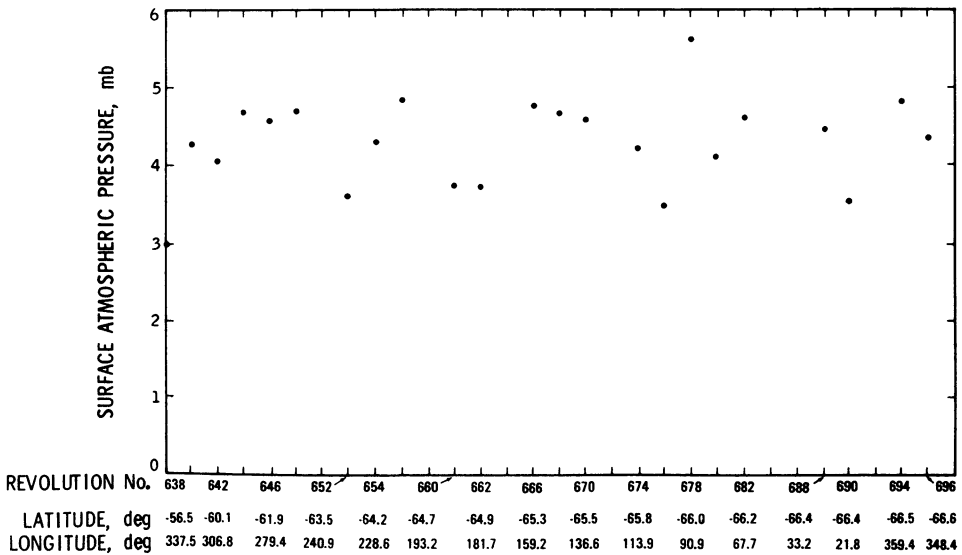


Fig. 16. Surface atmospheric pressures from Extended Mission II entry occultation measurements.

3. Topography

Topographical information is obtained from radio occultation data through the precise measurement of the radius of closest approach of the refracted radio beam. This is made possible by the precise timing of the occultation event, accurate knowledge of the ephemeris of the spacecraft near the time of occultation, and the inversion of the phase changes due to refraction to obtain the refractivity profile. The timing of the occultation is established by analyzing a spectrum of the signal at intervals sufficient to provide an adequate signal-to-noise ratio in the spectrum, and by performing an interpolation to obtain the point in time when the signal is approximately 6 dB below its normal pre-occultation value. This value corresponds closely to the value expected in the Fresnel pattern produced by a knife edge when the source is directly behind the edge. During the Standard Mission the signal-to-noise ratio was sufficient to analyze the signal spectrum at intervals of 0.068 s. During the Extended Missions, the signal-to-noise ratio had deteriorated to the point where 0.68 s sample intervals were required, and hence the uncertainty was greater by about an order magnitude. The ephemeris of the spacecraft at the time of occultation was obtained from precise determination of the orbit. It was estimated that the uncertainty in the time of periapsis passage was less than 0.1 s during the Standard Mission and may have been as large as 0.6 s during the Extended Missions. Hence, under the assumption that the uncertainties in occultation timing and of the trajectory time are independent, one obtains a timing uncertainty for the Standard Mission of about 0.1 s and for the Extended Missions about 0.9 s. The timing uncertainty maps into radius error through the magnitude of the radial velocity of the radio beam with respect to the surface of Mars. During the Standard Mission, the radial velocity was less than 2.5 km s^{-1} , and hence, the radius uncertainty due to timing was less than 0.25 km. During the first Extended Mission, the radial velocity was about 1 km s^{-1} , thus yielding a radius error of about 0.9 km. During the second Extended Mission in September and October of 1972, the timing uncertainty was still 0.9 s, but the velocity of the beam had increased about 2.3 km s^{-1} , resulting in a total radius error of about 2.1 km.

The first two Mars radius measurements with Mariner IV showed radii different by about 5 km, at roughly corresponding north and south latitudes, which immediately indicated the presence of large topographic elevation differences on Mars. Mariner VI and Mariner VII provided four more radius measurements, including measurements near the equator and the North Pole. These six points were then used to produce an oblate spheroid approximation to the physical shape of Mars, having an equatorial radius of 3394.5 km and a polar radius of 3378.2 km, for a flattening of 0.0048 (Kliore, 1971).

The large number of radius measurements taken with Mariner IX has provided much significant information on Martian global topography. The Standard Mission provided radius as well as pressure altitude measurements in the south equatorial regions and a narrow band of latitudes along 65° latitude. Altitudes in the south

equatorial region ranged from about -4.4 km in Hellas to a high of 9.6 km in Claritas, with a net excursion of 14 km and a mean altitude of 2.7 km referred to the 6.1 mb pressure level. The measurements in the vicinity of 65° latitude showed uniformly negative altitudes with a mean of -2.6 km. This disparity in surface pressure and elevation between the equatorial and circumpolar regions at first was thought to indicate that the physical shape of Mars was more oblate than the shape of a gravitational equipotential surface, or a geoid, leading to higher atmospheric pressures at high latitudes than at the equator. This implication was supported by a comparison of a triaxial ellipsoids which were fit to the first raw radius data from the Standard Mission, and then to radii of the 6.1 mb pressure level, which were computed from the measured radii as well as the deduced surface pressures and temperature profiles (Cain *et al.*, 1972). The flattening coefficients obtained from an average equatorial radius were 0.0074 in the case of the physical surface ellipsoid, and 0.0051 for the 6.1 mb isobaric surface, which was in fairly good agreement with the dynamical flattening of 0.005238 , obtained from the motion of the natural satellite of Mars (Sinclair, 1972).

Occultation measurements were taken near the North Pole during Extended Mission I, and it was found that the radii at these locations averaged to about 3377.8 km, indicating that the radius of Mars only changes by about 2 km from a latitude of 65° to the North Pole. These radii were also consistent with exit measurement of Mariner 6 (Kliore *et al.*, 1969, 1971). Thus it is obvious that the region around 65° latitude is substantially and systematically lower than other areas on Mars. In addition, all locations of occultation measurements in the northern hemisphere in Aetheria, Phlegra, and Amazonis exhibited altitudes from 1 to 3 km below the 6.1 mb isobaric level. However, when the measurements crossed into the Tharsis area (Figure 6) the elevations rose and the surface pressures dropped proportionately. Measurement points 432 and 436, lying on the Tharsis plateau, indicated pressure altitudes of about 6.7 km and measurement 438 taken on the 'Chandelier' region of the Coprates canyon indicates a pressure altitude of about 10 km and a surface pressure of 2 mb.

By coincidence, the location of measurement 434 entry fell very close to the top of the volcanic feature known as Middle Spot (Pavonis Mons), which was one of the four prominent features first discovered in Mariner IX television pictures during the Martian dust storm (Masursky *et al.*, 1972). Although the location of the occultation tangency point did not fall within the caldera of the volcano, the geometry was such that the line of sight practically bisected the entire volcanic shield, thus making it virtually certain that the beam was actually intercepted by the highest feature along the track, which is likely to have been the summit area. The radius that was measured here was 3417.1 km which is about 13.6 to 13.8 km above adjacent occultation measurements. On the basis of pressure altitudes, the height of Middle Spot was 12.5 km, and the pressure at the top was about 1 mb.

The entire southern hemisphere of Mars was found to be 3 to 4 km higher than corresponding latitudes in the northern hemisphere and the South polar area was

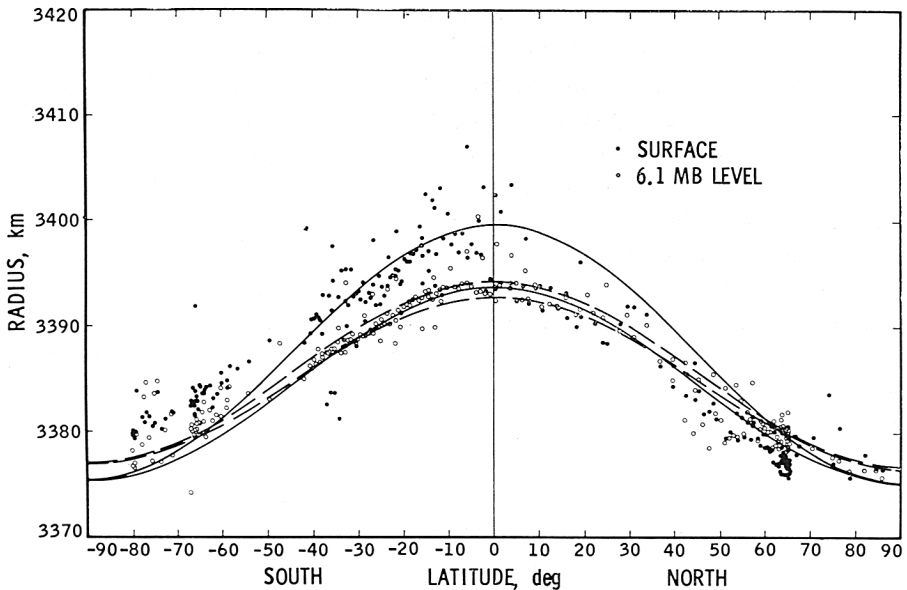


Fig. 17. Occultation radii measured by Mariner IX. The closed circles indicate radii of the solid surface and the open circles are derived radii of the 6.1 mb pressure level. The solid and dashed lines define the radii of fitted tri-axial ellipsoids approximating the solid surface and a 6.1 mb isobaric surface, respectively.

found to be higher than the North Pole by about 3.4 km. This asymmetry is obvious from an examination of Figure 17 which shows the measured radii of the solid surface, (solid dots) and the 6.1 mb level, (open dots) plotted vs the latitude of measurement. The solid lines show the maximum and minimum radii of an ellipsoid fitted to the measured solid radius data. The parameters of this ellipsoid are: A (major equatorial axis) = 3400.12 km; B (minor equatorial axis) = 3394.19 km; and C (polar axis) = 3375.45. The longitude of the major axis is 99.57° W. The broken lines represent radii of a triaxial ellipsoid fitted to the 6.1 mb level radii. For this ellipsoid $A = 3396.67$ km; $B = 3395.23$ km, $C = 3377.22$, and $\theta = 108.1^\circ$ W (Cain *et al.*, 1973). It is immediately obvious that radii measured in the southern hemisphere are obviously and systematically displaced about the upper limit of the triaxial ellipsoid, with the exception of four points in Hellas, which lie below the ellipsoid boundaries. At the same time, all northern hemisphere measurements, with the exception of a few points near the North Pole, lie within or below the ellipsoid boundaries. In particular, the large concentration of measurements at 65° and -65° latitudes clearly illustrate the asymmetry between the two hemispheres of Mars. In contrast, the 6.1 mb radii cluster fairly closely around the contours of their ellipsoid, with the exception of a few measurements in the southern hemisphere which were undoubtedly affected by the poor quality of the one-way data. It should be pointed out that the flattening corresponding to the solid surface ellipsoid is 0.0064 compared to a flattening for the 6.1 mb ellipsoid of 0.0055.

It is clear from the previous discussion that a triaxial ellipsoid is not a very good approximation for the physical surface of Mars. For that reason, models using a spherical harmonic representation were used to portray the shape of Mars (Cain *et al.*, 1973). For a second order spherical harmonic approximation, the best fit is displaced southward from the mass center by 2.85 km and there is an equatorial displacement of about 1.7 km in the direction of about 100° W. The resulting mean equatorial and polar radii are 3400.6 km and 3379.6 km, giving a flattening of 0.00607.

A spherical harmonic fit was also performed with the 6.1 mb isobaric radii. The resulting surface should correspond to a geoid, but only under quiescent conditions. Care must be taken in the interpretation of the isobaric data derived from the occultation experiment, because of the unknown effects of dynamical processes in the Martian atmosphere as well as seasonal effects upon the global atmospheric pressure of Mars. When an attempt was made to compare pressures referred to a gravitationally determined geoid of Mars in the circumpolar and the south equatorial regions, somewhat higher pressures than expected were noted in the circumpolar region, possibly indicating the effect of dynamical processes.

4. Conclusions and Recommendations

From the radio occultation results produced by Mariner IV, VI and VII and especially Mariner IX, several conclusions can be drawn regarding the nature and structure of the atmosphere and surface of Mars:

(1) The structure of the atmospheric temperature profiles in the daytime are quite sensitive to the presence of dust in the atmosphere, and thus could be used to gauge the relative clarity of the Martian lower atmosphere. For example, the nearly isothermal temperature profile obtained from the Mariner IV daytime measurement may indicate the presence of substantial dust in the atmosphere, which could partially explain the low contrast of the Mariner IV television pictures.

(2) Temperature gradients obtained from occultation measurements by Mariners VI, VII and IX while the atmosphere was apparently clear of dust, do not approach the adiabatic gradient predicted by theory for a clear Martian atmosphere in radiative-convective balance. It may be suggested that the vertical temperature structure in the daytime atmosphere of Mars is strongly modified by dynamical processes.

(3) The surface atmospheric pressure on Mars changes very drastically from one location on Mars to another in correspondence with changes in the topography. For example, pressure from about 10.3 mb in the North circumpolar region down to about 1 mb near the top of the Middle Spot volcano have been measured. In the near equatorial regions, the relative elevation difference between the Tharsis plateau and the Hellas basin amounts to some 20 km.

(4) The main peak of the daytime ionosphere behaves like a F_1 type layer produced by photoionization of carbon dioxide by extreme solar ultraviolet, with a subsidiary peak, possibly of the E -type, produced by solar X-rays.

(5) The physical body of Mars displays very pronounced equatorial and north-

south asymmetries, amounting to about 5 km and 3.5 km, respectively, thus rendering a simple triaxial figure representation impractical, and calling for more sophisticated spherical harmonic modelling.

(6) An isobaric surface derived from occultation data does not precisely agree with a geoid figure derived from spacecraft tracking data, indicating the presence of possible atmospheric dynamical effects upon the surface pressure.

The experience of the Mariner IV, VI, VII and IX radio occultation experiments have suggested several possible improvements in spacecraft radio system design that would greatly improve the quality of radio occultation data. Among these are the following:

(a) A stable spacecraft oscillator with a short-term stability of about 1 part in 10^{11} would almost double the amount of radio occultation data for any given mission by improving the quality of the one-way exit data to the level of the two-way entry data.

(b) The presence of a second coherent downlink frequency would enable the unambiguous separation of charged particles from a neutral atmosphere. Such a system will be flown on the Viking orbiters in 1975–76.

(c) A steerable spacecraft high gain antenna and an expanded attitude control system would extend the lifetime of the spacecraft useful for radio occultation measurements and would provide data on possible seasonal changes in atmospheric surface pressures.

Acknowledgements

The author gratefully acknowledges the help of colleagues and associates who have contributed to the success of the Mariner Radio Occultation Experiments. These include: T. W. Hamilton, D. L. Cain, G. Fjeldbo, B. L. Seidel, G. S. Levy, S. I. Rasool, J. F. Jordan, M. J. Sykes, P. M. Woiceshyn, and various Mariner project personnel at JPL as well as NASA, together with the personnel of the Deep Space Net. The majority of the work described in this paper was performed at the Jet Propulsion Laboratory, under NASA Contract NAS 7-100 and at Stanford University under NASA grant NGR 05-020-065.

References

- Barth, C. A., Stewart, A. I., Hord, C. W., and Lane, A. L.: 1972, *Icarus* **17**, 457.
 Bean, B. R. and Thayer, G. D.: 1963, *J. Res. NBS-D; Radio Propagation* **07D**, No. 3, 273.
 Cain, D. L., Kliore, A. J., Seidel, B. L., and Sykes, M. J.: 1972, *Icarus* **17**, 517.
 Cain, D. L., Kliore, A. J., Seidel, B. L., Sykes, M. J., and Woiceshyn, P. M.: 1973, *J. Geophys. Res.* **78**, 4352.
 Fjeldbo, G.: 1964, Report SU-SEL-64-025, Stanford Electronics Laboratories, Stanford, California.
 Fjeldbo, G. and Eshleman, V. R.: 1968, *Planetary Space Sci.* **16**, 1035.
 Fjeldbo, G., Kliore, A., and Seidel, B.: 1970, *Radio Sci.* **5**, 381.
 Gierasch, P. and Goody, R.: 1968, *Planetary Space Sci.* **16**, 615.
 Kieffer, H. H.: 1972, private communication.
 Kliore, A. J., Cain, D. L., and Hamilton, T. W.: 1964, JPL-TR-32-674, Jet Propulsion Laboratory, Pasadena, Calif.
 Kliore, A. J., Cain, D. L., Levy, G. S., Eshleman, V. R., Drake, F. D., and Fjeldbo, G.: 1965a, *Astron. Aeron.* **7**, 72.
 Kliore, A. J., Cain, D. L., Levy, G. S., Eshleman, V. R., Fjeldbo, G., and Drake, F. D.: 1965b, *Science* **149**, 1243.

- Kliore, A. J., Cain, D. L., Levy, G. S.: 1968, in *Space Research VII, Moon and Planets*, North Holland Publishing Company, Amsterdam, p. 220.
- Kliore, A. J., Fjeldbo, G., Seidel, B. L., and Rasool, S. I.: 1969, *Science* **166**, 1393.
- Kliore, A. J., Cain, D. L., Seidel, B. L., and Fjeldbo, G.: 1970a, *Icarus* **12**, 82.
- Kliore, A. J., Fjeldbo, G., and Seidel, B. L.: 1970b, *Radio Sci.* **5**, 373.
- Kliore, A. J.: 1971, *Bull. Am. Astron. Soc.* **3**, 498 (abstract).
- Kliore, A. J., Fjeldbo, G., and Seidel, B. L.: 1971, *Space Research* **10**, 165.
- Kliore, A. J.: 1972, in L. Colin (ed.), *Proc. Workshop on the Mathematics of Profile Inversion*, NASA TM-X-62, 150, 3-2, 3-16.
- Kliore, A. J., Cain, D. L., Fjeldbo, G., Seidel, B. L., and Rasool, S. I.: 1972a, *Science* **175**, 313.
- Kliore, A. J., Cain, D. L., Fjeldbo, G., Seidel, B. L., Sykes, M. J., and Rasool, S. I.: 1972b, *Icarus* **17**, 484.
- Kliore, A. J., Fjeldbo, G., Seidel, B. L., Sykes, M. J., and Woiceshyn, P. M.: 1973, *J. Geophys. Res.* **78**, 4331.
- KolosoV, M. A., Yakovlev, O. I., Kruglov, Yu. M., Trusov, B. P., Yefimov, A. I., and Kerzhanovich, V. V.: 1972, *Radiotekhnika i Elektronika* **12**, 2483 (in Russian).
- Masursky, H., *et al.*: 1972, *Science* **174**, 1321.
- Rasool, S. I., Hogan, J. S., Stewart, R. W., and Russell, L. H.: 1970, *J. Atmospheric Sci.* **27**, 841.
- Sinclair, A. T.: 1972, *Monthly Notices Roy. Astron. Soc.* **155**, 249.
- Stone, P. H.: 1972, *J. Atmospheric Sci.* **29**, 405.

DISCUSSION

Pearl: I have two comments. First, such strong temperature inversions as you suggest over the north polar cap have terrestrial analogs: such inversions are observed in the antarctic. Secondly, computations based on Mariner 9 IRIS temperature profile data indicate that 15–20% of the incident solar radiation is absorbed by the dusty atmosphere during the dust storm.